

## Probing the Pharmacophore of Ginkgolides as Glycine Receptor Antagonists

Anders A. Jensen,<sup>\*,†</sup> Nasreen Begum,<sup>‡</sup> Stine B. Vogensen,<sup>†</sup> Kolja M. Knapp,<sup>†</sup> Klaus Gundertofte,<sup>‡</sup> Sergei V. Dzyuba,<sup>§</sup> Hideki Ishii,<sup>§</sup> Koji Nakanishi,<sup>§</sup> Uffe Kristiansen,<sup>‡</sup> and Kristian Strømgaard<sup>\*,†</sup>

Departments of Medicinal Chemistry and Pharmacology & Pharmacotherapy, The Faculty of Pharmaceutical Sciences, University of Copenhagen, Universitetsparken 2, DK-2100 Copenhagen, Denmark, Department of Computational Chemistry, H. Lundbeck A/S, Ottiliavej 7-9, DK-2500 Valby, Denmark, and Department of Chemistry, Columbia University, 3000 Broadway, New York, New York 10027

Received January 2, 2007

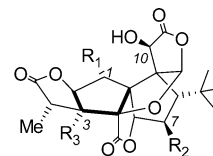
Ginkgolides are antagonists of the inhibitory ligand-gated ion channels for the neurotransmitters glycine and  $\gamma$ -aminobutyric acid (GABA). In this study the ginkgolide structure was modified in order to investigate the minimum structural requirements for glycine receptor antagonism. The five native ginkgolides and a series of 29 ginkgolide derivatives were characterized at the three glycine receptor subtypes  $\alpha 1$ ,  $\alpha 1\beta$ , and  $\alpha 2$ , which revealed that only minor changes in the ginkgolide skeleton were allowed for maintaining glycine receptor antagonism. A pharmacophore model was generated and applied in a virtual screening of a compound database (300 000 compounds), resulting in the identification of 31 hits. Twenty-seven of these hits were screened for biological activity, but none displayed antagonist activity at the glycine receptors. This strongly suggests the importance of other pharmacophore components in the binding of ginkgolides to glycine receptors, and we propose that the structural rigidity of the ginkgolide molecule may be crucial for its glycine receptor activity.

### Introduction

The *Ginkgo biloba* tree is among the oldest living plants and is referred to as a “living fossil”. The Ginkgo tree has a long history of use in traditional Chinese medicine, but it was not until the 1960s that a standardized extract of *G. biloba* leaves, EGb 761, was introduced into the European markets.<sup>1</sup> Today *G. biloba* extract is one of the most popular herbal medicines worldwide.

Numerous beneficial effects of EGb 761 have been proposed over the years. The extract has been claimed capable of improving peripheral vascular function, inhibiting thrombosis and embolism, being neuroprotective in Alzheimer’s disease and cognitive disorders, and possessing antiinflammatory, antiproliferative, and antioxidant activities.<sup>2</sup> EGb 761 is a complex mixture of compounds, the main ingredients being flavonoids (24%) and terpene trilactones (ginkgolides and bilobalide, 6%).<sup>3</sup> It is believed that the flavonoids predominantly act as antioxidants, whereas the terpene trilactones are involved in antiinflammation and prevention of blood clotting, an effect associated with the antagonistic activity of the ginkgolides at the platelet-activating factor (PAF) receptor.<sup>4</sup> In contrast, the neuroprotective effects of EGb 761 have so far not been unequivocally linked to specific components of the extract, although effects from terpene trilactones have been demonstrated.<sup>5,6</sup>

The ginkgolides are unique components of EGb 761, and the compounds are characterized by a cage-like skeleton consisting of six five-membered rings, i.e., a spiro[4.4]nonane carbocyclic ring, three lactones, and a tetrahydrofuran moiety (Figure 1).<sup>7</sup> In contrast to many studies of the neuroprotective effects of EGb 761, the isolated ginkgolides have not been extensively



	R <sub>1</sub>	R <sub>2</sub>	R <sub>3</sub>
ginkgolide A (GA, <b>1</b> )	H	H	OH
ginkgolide B (GB, <b>2</b> )	OH	H	OH
ginkgolide C (GC, <b>3</b> )	OH	OH	OH
ginkgolide J (GJ, <b>4</b> )	H	OH	OH
ginkgolide M (GM, <b>5</b> )	OH	OH	H

**Figure 1.** Structure of the native ginkgolides A, B, C, J, and M, which differ by the position and the number of hydroxyl groups in positions 1, 3, and 7.

studied, partly due to limited availability of pure ginkgolides. When ginkgolide B (GB, **2**) was found to be a potent antagonist of the PAF receptor in 1985, extensive structure–activity relationship (SAR) studies of ginkgolides for this receptor were performed.<sup>8</sup> However, the significance of the PAF receptor-component for the neuroprotective effects of EGb 761 is not well understood.

In an attempt to search for novel targets for ginkgolides, radiolabeled versions of ginkgolides have been prepared including [<sup>3</sup>H]- and [<sup>18</sup>F]-labeled GB.<sup>9,10</sup> Although biodistribution studies in rats using [<sup>3</sup>H]-GB showed that GB (**2**) entered the brain, the amounts detected in the brain by positron emission tomography (PET) using [<sup>18</sup>F]-GB was too low to be unambiguously determined.<sup>11</sup> Instead, the first indication of a direct interaction between ginkgolides and important targets in the brain was discovered, when ginkgolides were shown to be potent and highly selective antagonists of the inhibitory strychnine-sensitive glycine receptor (GlyR).<sup>12–14</sup> The GlyRs are ligand-gated ion channels found primarily in the spinal cord and brain stem, but also in higher brain regions such as the hippocampus

\* To whom correspondence should be addressed. A.A.J.: Phone +45 3530 6491. Fax: (+45) 35306040. E-mail: aaj@farma.ku.dk. K.S.: Phone +45 3530 6114. Fax: (+45) 35306040. E-mail: krst@farma.ku.dk.

<sup>†</sup> Department of Medicinal Chemistry, Faculty of Pharmaceutical Sciences, University of Copenhagen.

<sup>‡</sup> Department of Pharmacology & Pharmacotherapy, Faculty of Pharmaceutical Sciences, University of Copenhagen.

<sup>§</sup> Columbia University.

<sup>1</sup> H. Lundbeck A/S.

<sup>a</sup> Abbreviations: FMP, FLIPR membrane potential; GA, ginkgolide A; GB, ginkgolide B; GC, ginkgolide C; GJ, ginkgolide J; GM, ginkgolide M; GlyR, glycine receptor.

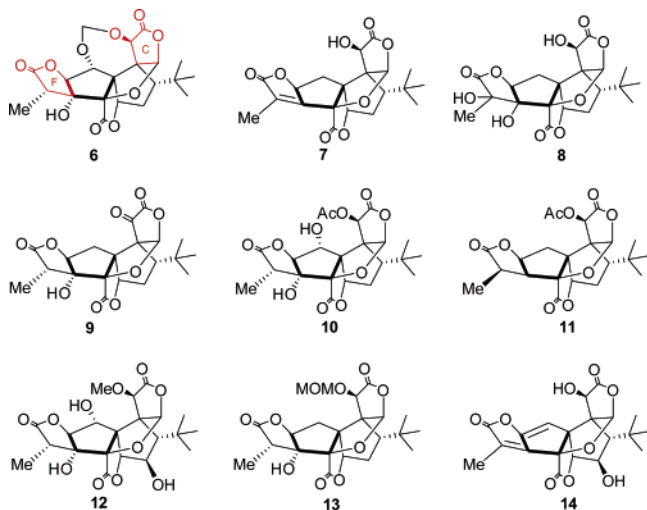


**Figure 2.** Ginkgolide derivatives, where the two lactones C and F are intact, while derivatizations are made in various positions.

and developing cortex. The receptors are protein complexes composed of five subunits, either as homomeric receptors consisting of five identical  $\alpha$  subunits ( $\alpha 1$ – $\alpha 4$ ) or as heteromeric complexes containing  $\alpha$  and  $\beta$  subunits.<sup>15,16</sup> The neuropharmacology and functional importance of GlyRs in higher brain regions is not well characterized, which in part can be attributed to the lack of potent and selective ligands for the receptors.<sup>17</sup> In addition to their effect at GlyRs, ginkgolides are also moderately potent antagonists of the structurally and functionally related  $\gamma$ -aminobutyric acid (GABA<sub>A</sub>) receptors.<sup>14</sup>

Since the discovery of the GABA<sub>A</sub> and glycine receptor antagonism displayed by ginkgolides, a number of studies have investigated these effects in more detail. Kondratskaya et al. have recently provided evidence for ginkgolides having preferential activity at heteromeric GlyRs over homomeric GlyRs<sup>18,19</sup> in contrast to picrotoxinin, which is a fairly selective antagonist of homomeric GlyRs. Moreover, the ginkgolides were shown to be sensitive to mutations in the pore-forming M2 segment of the GlyR, thereby supporting the idea of ginkgolides as open-channel blockers. Very recently, Lynch and co-workers have substantiated the finding that ginkgolides bind to the pore-forming region and showed that they most likely bind to two residues in the M2 segment.<sup>20</sup>

In a study of the effects of ginkgolides at recombinant  $\alpha 1\beta 2\gamma 2L$  GABA<sub>A</sub> receptors, GA, GB, and GC (**1–3**) were found to be noncompetitive antagonists with IC<sub>50</sub> values around 10  $\mu$ M.<sup>21</sup> Finally, in another study at native GlyRs in cultured hippocampal neurons,<sup>22</sup> GB (**2**) and GC (**3**) were found to be the most potent ginkgolides with IC<sub>50</sub> values of 273 and 267 nM, respectively. In contrast, little or no biological activity of

ginkgolides was observed for these compounds at GABA<sub>C</sub> and ionotropic glutamate receptors.<sup>22</sup>

In a previous SAR study of ginkgolide derivatives and their antagonism of GlyRs, it was shown that ether, ester, and carbamoyl substitutions at any hydroxyl group in GC (**3**) led to a dramatic decrease in GlyR activity.<sup>23</sup> In the present study another approach has been taken: introducing more subtle changes of the ginkgolide molecule, particularly reduction and/or decomposition of the native structure, hoping that this will provide information on the minimal structural requirements for biological activity at the GlyRs. Thus, the aim of this study was to determine these requirements by functional characterization of ginkgolide derivatives at different GlyR subtypes and apply this information in the search for alternative structures possessing similar GlyR antagonistic activities.

## Chemistry

Five different ginkgolides, ginkgolides A, B, C, J, and M (**1–5**, Figure 1) are found in the *G. biloba* tree, which have the same carbocyclic skeleton, but differ in numbers and positions of hydroxyl groups. In a previous study the two lactones C and F in the ginkgolide molecules (Figure 2) were proposed to be important determinants for the GlyR inhibition based on molecular modeling and a comparison with picrotoxin, which has a similar 3D structure.<sup>14</sup> Therefore, we were particularly interested in investigating the effects of modifying these regions of the ginkgolides, and a range of derivatives were selected to test this hypothesis. Furthermore, derivatives were selected that could expand the general SAR for ginkgolides as GlyR antagonists.

The ginkgolide derivatives in this study can be categorized into four groups based on their structural modifications: In one group, lactones C and F were intact, while a number of other modifications were introduced in the ginkgolide molecule (Figure 2). These modifications include selective oxidation of 10-OH (**9**, Figure 2), substitution of the 10-OH group (**10–13**, Figure 2), and introduction of double bonds by elimination (**7** and **14**, Figure 2). In another group either lactone C was opened (**15**, Figure 3) or removed (**16** and **17**, Figure 3) or lactone F was modified (**18–21**, Figure 3), while the remaining lactones were intact. In order to more specifically address the function of the carbonyl group of these lactones, a series of GA (**1**) derivatives were prepared where the carbonyl functionality was consecutively removed. First the carbonyl group of lactone F was selectively reduced (**22**, Figure 4), followed by reduction of lactone C (**23**, Figure 4), and finally the fully reduced analogue (**24**, Figure 4) was obtained. The final group of ginkgolide derivatives under investigation were those where the 7-position was modified, and a number of functionalities were

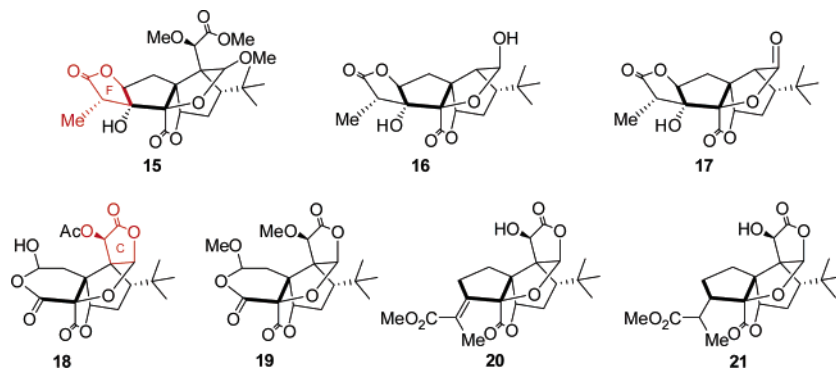


**Figure 3.** Ginkgolide derivatives where lactones C and F are perturbed.

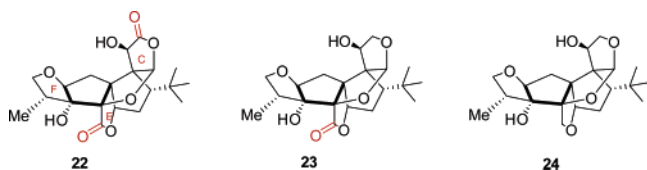


**Figure 4.** Systematic reduction of the carbonyl group of the lactones in ginkgolide A.

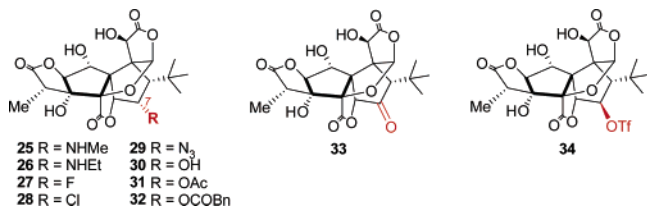


**Figure 5.** Ginkgolide B derivatives with substituents in the 7-position.

introduced (**25–32** and **34** Figure 5), as well as oxidation of the 7-OH to the carbonyl group (**33**, Figure 5).

Generally, all the compounds investigated were either from previous studies or prepared according to previously published procedures. The nine compounds listed in Figure 2 were either available in our laboratories from previous studies (compounds **6**, **8**, **9**, **11**),<sup>24–27</sup> or prepared according to literature procedures (compounds **7**,<sup>28</sup> **10**,<sup>29</sup> **12**,<sup>26</sup> **13**,<sup>26</sup> and **14**).<sup>25</sup> All the compounds (**15–21**) in Figure 3 were available in our laboratories from previous studies.<sup>24–27</sup> Compounds **22–24** (Figure 4) were recently synthesized by a selective reduction of GA (**1**) using DIBAL-H followed by a deoxygenation of the lactols by treatment with Et<sub>3</sub>SiH–BF<sub>3</sub>·Et<sub>2</sub>O to form the corresponding tetrahydrofuran moieties.<sup>30</sup> The 7-substituted ginkgolide derivatives (Figure 5) were prepared by Vogensen et al.<sup>31</sup> Initially GC (**3**) was reacted with trifluoromethanesulfonyl (Tf) anhydride to provide 7β-OTf-GB (**34**), which could be reacted with a range of nucleophiles to provide compounds **25–32**.<sup>31</sup> The oxidized derivative, compound **33**, was obtained by treatment of GC (**3**) with CrO<sub>3</sub>, as previously described by Corey and co-workers.<sup>32</sup>

## In Vitro Pharmacology

**Functional Characterization of Native Ginkgolides and Derivatives at α1, αβ, and α2 GlyRs in the FMP Assay.** The functional properties of the five native ginkgolides GA (**1**), GB (**2**), GC (**3**), GJ (**4**), and GM (**5**) as well as the 29 ginkgolide derivatives were evaluated using HEK293 cell lines expressing the human GlyR subtypes α1, α1β, and α2 using the FLIPR Membrane Potential (FMP) assay. The pharmacological characteristics of the three cell lines have been investigated in previous studies.<sup>33,34</sup> The potencies of agonists and antagonists in the FMP assay were found to be slightly lower than those found in conventional electrophysiological set-ups. However, the rank orders of EC<sub>50</sub>, K<sub>i</sub>, and IC<sub>50</sub> values of a wide range of standard GlyR ligands obtained in the assay were in accordance with those obtained in electrophysiology studies.<sup>33,34</sup>

In previous studies, glycine exhibited EC<sub>50</sub> values of approximately 100 μM, 100 μM, and 300 μM at the α1, α1β, and α2 GlyR-cell lines, respectively.<sup>33,34</sup> Hence, in this study we used EC<sub>70</sub>–EC<sub>90</sub> glycine concentrations of 200 μM, 200 μM, and 500 μM for the pharmacological characterization of the ginkgolides at the α1, α1β, and α2 receptor subtypes, respectively. Since ginkgolides have been shown to be uncompetitive antagonists of the GlyRs,<sup>18</sup> small differences in effective agonist concentrations should not influence the determined IC<sub>50</sub> values of the compounds. The IC<sub>50</sub> values for the native ginkgolides and the 29 derivatives are given in Table 1. The

**Table 1.** Functional Properties of Native Ginkgolides and Ginkgolide Analogues at Human α1, α1β, and α2 GlyR-HEK293 Cell Lines in the FMP Assay<sup>a</sup>

compd	IC <sub>50</sub> (μM)		
	α1	α1β	α2
GA ( <b>1</b> )	1.9 [5.7 ± 0.03]	0.69 [6.2 ± 0.04]	2.1 [5.7 ± 0.04]
GB ( <b>2</b> )	2.9 [5.5 ± 0.04]	2.1 [5.7 ± 0.04]	3.7 [5.4 ± 0.05]
GC ( <b>3</b> )	4.7 [5.3 ± 0.02]	2.4 [5.6 ± 0.03]	8.2 [5.1 ± 0.04]
GJ ( <b>4</b> )	7.1 [5.1 ± 0.03]	4.2 [5.4 ± 0.05]	12 [4.9 ± 0.02]
GM ( <b>5</b> )	0.78 [6.1 ± 0.03]	0.56 [6.3 ± 0.03]	1.3 [5.9 ± 0.04]
<b>6</b>	12 [4.9 ± 0.05]	8.9 [5.1 ± 0.03]	12 [4.9 ± 0.03]
<b>7</b>	6.2 [5.2 ± 0.04]	3.1 [5.5 ± 0.04]	9.5 [5.0 ± 0.06]
<b>12</b>	9.8 [5.0 ± 0.04]	5.2 [5.3 ± 0.02]	7.8 [5.1 ± 0.05]
<b>27</b>	7.3 [5.1 ± 0.05]	3.2 [5.5 ± 0.03]	4.6 [5.3 ± 0.03]
<b>28</b>	7.6 [5.1 ± 0.03]	3.2 [5.5 ± 0.04]	13 [4.9 ± 0.04]
<b>29</b>	17 [4.8 ± 0.02]	7.4 [5.1 ± 0.04]	29 [4.5 ± 0.07]

<sup>a</sup> The data are means of 3–8 individual experiments. The ginkgolide analogues **8–11**, **13–26**, and **30–34** displayed IC<sub>50</sub> values >100 μM at all three GlyR subtypes. The IC<sub>50</sub> values of the compounds are given in μM with pIC<sub>50</sub> ± SEM in brackets.

five native ginkgolides and six of the derivatives exhibited IC<sub>50</sub> values in the high nanomolar to mid-micromolar range (Figure 6), whereas the remaining 23 ginkgolide derivatives were found to be inactive at concentrations up to 100 μM.

**Electrophysiological Characterization of Native Ginkgolides at α1 GlyRs.** In addition to FMP assay, native ginkgolides were investigated by electrophysiology using the patch-clamp technique. The five native ginkgolides were evaluated using the same cells as described above, although only the homomeric α1 GlyR subtype was studied.

Initially the concentration–response for glycine was established, showing an EC<sub>50</sub> of 88 μM [77,101] and a Hill coefficient of 2.1 [1.5; 2.8] (95% confidence intervals in brackets, *n* = 10–11 cells). From this a concentration of 300 μM glycine, corresponding to approximately EC<sub>90</sub>, was chosen for the subsequent inhibition experiments with native ginkgolides (Figure 7). The parameters describing each ginkgolide are summarized in Table 2. For all ginkgolides, the Hill coefficients of the concentration–inhibition relationships were not significantly different from 1.

In order to investigate the nature of ginkgolide antagonism of glycine-induced currents in more detail, concentration–inhibition experiments with GC (**3**) and two additional concentrations of glycine (30 and 3000 μM) were carried out (Figure 8). IC<sub>50</sub> values were 2.4 μM [1.9; 3.0], 1.2 μM [1.0; 1.3], and 5.9 μM [4.5; 7.8] with 30, 300, and 3000 μM glycine, respectively, and the corresponding Hill coefficients were 0.87 [0.70; 1.04], 1.1 [0.93; 1.3], and 0.79 [0.61; 0.96], respectively (mean values of 5 cells with 95% confidence intervals in brackets). Even though the IC<sub>50</sub> values are significantly different, the results suggest a noncompetitive mode of action because the hallmark of competitive antagonism, a positive correlation between agonist concentration and IC<sub>50</sub>, is not present.

## Virtual Screening

A pharmacophore model was generated by overlaying the X-ray crystallographic structures of native ginkgolides GA (**1**) and GB (**2**) with the minimized structures of compounds GC (**3**) and GM (**5**) (Figure 9). The superimposition of these structures verified the rigidity of the ginkgolide structures, as the deviation among the structures in the core skeleton was minimal and functional groups were placed in very similar regions (Figure 9). The pharmacophore model was used as a template for a virtual screening of a library of ca. 300 000 compounds. The screening was carried out using Molecular

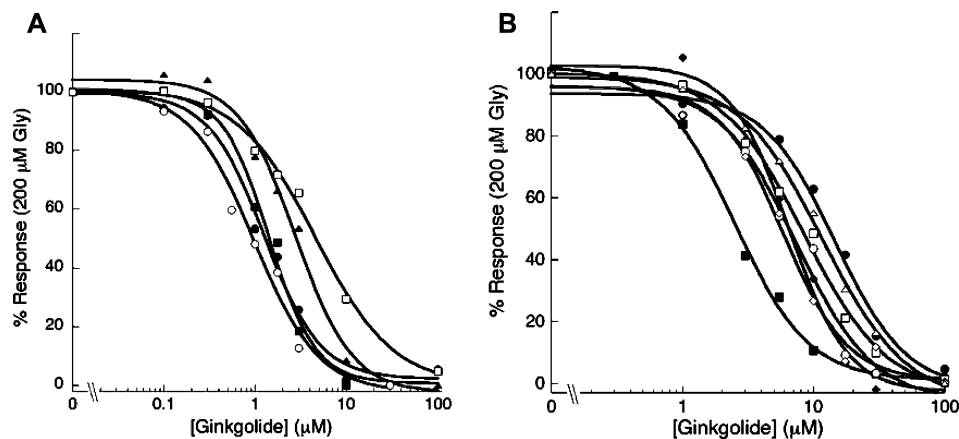


**Figure 6.** Functional profiles of native ginkgolides and ginkgolide analogues at human  $\alpha 1$  GlyR in the FMP assay. A. Concentration–response curves for native ginkgolides GA (■), GB (●), GC (▲), GJ (□), and GM (○) at the stable  $\alpha 1$  GlyR-HEK293 cell line using 200  $\mu\text{M}$  Gly as agonist concentration. B. Concentration–response curve for native ginkgolide GA (■) and ginkgolide analogues 6 (●), 7 (◆), 12 (□), 27 (○), 28 (◇), and 29 (△) at the stable  $\alpha 1$  GlyR-HEK293 cell line using 200  $\mu\text{M}$  Gly as agonist concentration. Error bars are omitted for reasons of clarity.

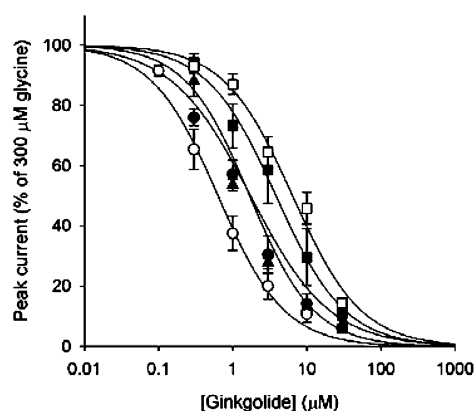


**Figure 7.** Inhibition by native ginkgolides GA (■), GB (●), GC (▲), GJ (□), and GM (○) of glycine-induced currents in human  $\alpha 1$  GlyR-HEK293 cells measured in whole-cell patch-clamp experiments. Glycine and varying concentrations of the ginkgolides were applied simultaneously to the cells. The response to 300  $\mu\text{M}$  glycine alone has been set as 100%, and the other responses are expressed as a fraction hereof. The response to glycine is progressively reduced with increasing concentrations of the ginkgolides. The number of cells tested in this way with each compound varied from five to seven.

**Table 2.** Inhibition by Native Ginkgolides of Glycine (300  $\mu\text{M}$ )-Induced Currents in Human  $\alpha 1$  GlyR-HEK293 Cells Measured in Whole-Cell Patch-Clamp Experiments<sup>a</sup>

compd	IC <sub>50</sub> ( $\mu\text{M}$ )	Hill coefficient
GA (1)	3.8 [2.6; 5.7]	0.93 [0.59; 1.27]
GB (2)	1.7 [1.2; 2.5]	0.81 [0.56; 1.06]
GC (3)	1.7 [1.2; 2.3]	1.00 [0.70; 1.31]
GJ (4)	6.4 [5.1; 8.2]	0.94 [0.73; 1.15]
GM (5)	0.65 [0.51; 0.84]	0.97 [0.74; 1.20]

<sup>a</sup> IC<sub>50</sub> values and Hill coefficients are given as means of 5–7 individual cells with 95% confidence intervals in brackets.

Operating Environment (MOE) and resulted in 31 hits. Twenty-seven of these hits were purchased and examined for GlyR activity in the FMP assay, which all showed IC<sub>50</sub> values > 100  $\mu\text{M}$ .

## Discussion

**Native Ginkgolides.** The rank order of the IC<sub>50</sub> values obtained for the native ginkgolides in the FMP assay was GJ  $\geq$  GC  $\geq$  GB  $\geq$  GA  $\geq$  GM (1–5) at all three GlyR subtypes. It is the first time the ginkgolide GM (5) has been evaluated on either recombinant or native GlyRs, and the compound was

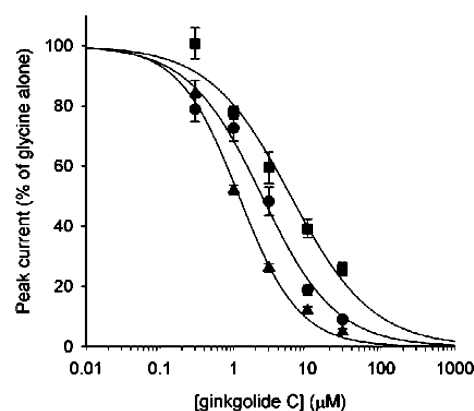


**Figure 8.** Effect of varying glycine concentrations on the inhibition by GC (3) in human  $\alpha 1$  GlyR-HEK293 cells measured in whole-cell patch-clamp experiments. 30 (●), 300 (▲), and 3000 (■)  $\mu\text{M}$  glycine and varying concentrations of GC (3) were applied simultaneously to the cells. The response of each glycine concentration alone has been set as 100%, and the other responses are expressed as a fraction hereof. Five cells were tested with each glycine concentration.

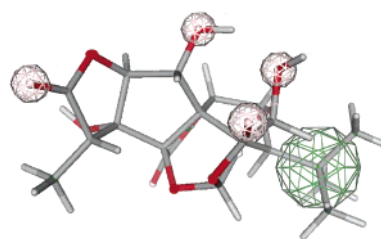


**Figure 9.** Query for virtual screening based on the developed pharmacophore model. Ginkgolide B (2) is aligned to query. Donor–acceptor functionalities shown in white, hydrophobic feature in green.

identified as the most potent GlyR antagonist of the five native ginkgolides. The differences between the antagonist potencies of the five ginkgolides were quite small, however, illustrated by the fact that GM (5) only displayed 8–9 fold lower IC<sub>50</sub> values at the three GlyR subtypes than the weakest antagonist of the native ginkgolides, GJ (4, Table 1). As previously observed for other GlyR antagonists,<sup>33,34</sup> the absolute IC<sub>50</sub> values for the five ginkgolides determined in the FMP assay were slightly higher than previously reported IC<sub>50</sub> values from studies of the compounds at recombinant GlyRs in conventional electrophysiological set-ups.<sup>18</sup> For example, GB (2) displayed IC<sub>50</sub> values of 2.9  $\mu\text{M}$ , 2.1  $\mu\text{M}$ , and 3.7  $\mu\text{M}$  at  $\alpha 1$ ,  $\alpha 1\beta$ , and  $\alpha 2$  GlyRs in the FMP assay (Table 1), whereas the same compound

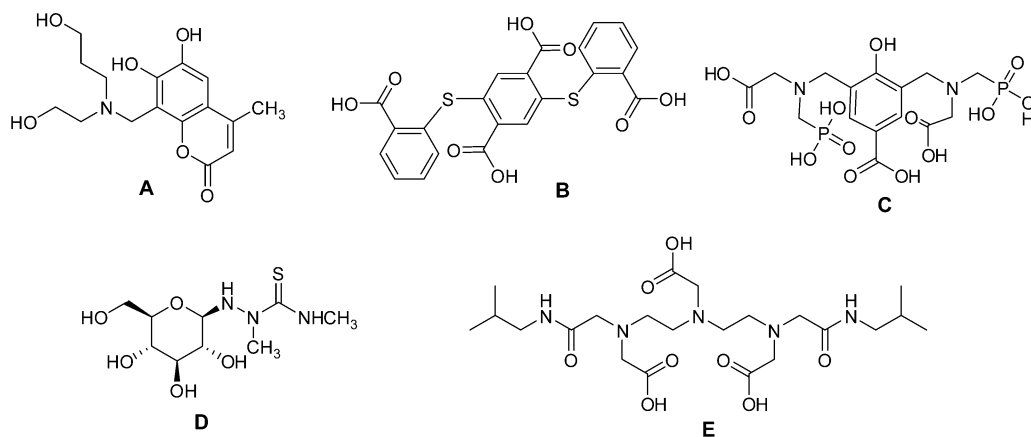


**Figure 10.** Representative structures, compounds A–E, of the 31 hits found in the virtual screening.

has exhibited  $IC_{50}$  values of  $0.61 \mu\text{M}$ ,  $0.18 \mu\text{M}$ , and  $3.7 \mu\text{M}$  at the respective receptors in *Xenopus* oocytes.<sup>18</sup> Furthermore, Kondratskaya et al. observed a 6-fold preference of GB (2) for the  $\alpha 1$  GlyR over the  $\alpha 2$  subtype and a 3-fold preference of the ginkgolide for the heteromeric  $\alpha 1\beta$  GlyR over the homomeric  $\alpha 1$  GlyR.<sup>18</sup> We did not observe these subtle subtype differences for GB (2) or any of the other four native ginkgolides in the FMP assay, which probably could be ascribed to the FMP assay being less sensitive than electrophysiological recordings (Table 1). On the other hand, the assay has been shown capable of detecting the well-documented preference of picrotoxin for the homomeric  $\alpha 1$  GlyR over the heteromeric  $\alpha 1\beta$  subtype.<sup>33,34</sup>

The functional pharmacology of the native ginkgolides was also studied in patch-clamp recordings on the  $\alpha 1$  GlyR-HEK293 cell line. The rank order of the antagonist potencies determined for the ginkgolides was in good agreement with that obtained in the FMP assay and in both cases GM (5) is the most potent ginkgolide. In the electrophysiological characterization GM (5) had an  $IC_{50}$  value of  $0.65 \mu\text{M}$ , while the four other native ginkgolides had  $IC_{50}$  values between  $1.7$  and  $6.4 \mu\text{M}$  (Table 2). In all cases Hill coefficients were around 1, indicating that ginkgolides bind GlyRs with a stoichiometry of 1:1.

It is noticeable that GM (5), which is investigated here for the first time, is the most potent ginkgolide in both pharmacological assays. Structurally GM (5) is characterized by lacking the 3-OH, in contrast to the other native ginkgolides (Figure 1), thus suggesting that the presence of a OH group in the 3-position is not favorable for GlyR activity.

**Ginkgolide Derivatives.** The 29 ginkgolide derivatives, compounds 6–34, were investigated in the FMP assay described above at the three different subunit combinations. Of the 29 derivatives, only six compounds showed activity, whereas the remaining 23 compounds displayed  $IC_{50}$  values  $> 100 \mu\text{M}$  at all three GlyR subtypes. The six compounds, 6, 7, 12, 27–29 with GlyR antagonistic activity were equipotent or less potent than the native ginkgolides, displaying  $IC_{50}$  values ranging from  $3.1$  to  $17 \mu\text{M}$  and generally not showing selectivity toward any of the three GlyR subtypes (Table 1).

In a previous SAR study of ginkgolides and GlyRs, we demonstrated that derivatization of the hydroxyl groups in the ginkgolide structure resulted in a dramatic decrease in GlyR activity.<sup>23</sup> In this study it is demonstrated that it is possible to modify ginkgolides and still maintain biological activity. Structurally the six derivatives that display activity at GlyRs divide into two distinctive classes, with compounds 6, 7, 12 being ginkgolides modified in lactone C or F (Figure 2), while compounds 27–29 are ginkgolides derivatized at position 7 (Figure 4). In all cases the modification must be considered

relatively modest, and this illustrates that GlyR activity is only retained with minor changes to the ginkgolide structure.

**Virtual Screening.** This study, as well as a previous study,<sup>23</sup> has demonstrated that enhancement of the antagonistic properties of ginkgolides at GlyRs is very difficult. Although some of the analogues presented in this study are almost equipotent with the native ginkgolides, so far it has not been possible to achieve increased activity beyond native ginkgolides. Moreover, the preparation of ginkgolide derivatives is far from trivial and is strongly dependent on the availability of native ginkgolides for derivatization. In a quest for potent and selective GlyR ligands, a pharmacophore model for the inhibition of GlyR by ginkgolides was generated. Application of this model in a virtual screening could be a way to circumvent the structural complexity of ginkgolides and discover structurally novel GlyR ligands. The strategy was considered particularly promising, as the ginkgolides are highly rigid structures; thus very few pharmacologically active conformations are possible.

The pharmacophore model was generated from the results obtained in this study, as well as results from a previous study,<sup>23</sup> and subsequently submitted for a virtual screening of 300 000 commercially available compounds. The screening resulted in 31 hits, and the structures of these hits were characterized by having several hydroxyl groups and/or carbonyl groups, thus mimicking the pharmacophore elements of the ginkgolides. However, in contrast to the ginkgolides most of the hits had much less rigid structures, as seen from the representative examples listed in Figure 10.

Twenty-seven compounds of the 31 hits including compounds A–E (Figure 10) were purchased and tested in the FMP assay (Supporting Information). All of the 27 compounds showed  $IC_{50}$  values  $> 100 \mu\text{M}$ . Thus, clearly the pharmacophore model does not fully contain the biologically relevant information for inhibition of GlyRs. Most importantly, the hits in the virtual screening were much more flexible structures than the ginkgolides, which themselves are quite rigid, cage-like structures. It is therefore tempting to speculate that the rigidity of the ginkgolide structures is crucial for their antagonistic activities at GlyRs.

## Conclusion

The native ginkgolides have been pharmacologically evaluated at three different GlyR combinations in a fluorescence-based high-throughput screening assay and at the  $\alpha 1$  homomeric GlyR in an electrophysiological assay. Generally there was a good agreement between the two assays. Interestingly, the studies showed that the native ginkgolide GM (5), which had not previously been characterized at GlyR, was the most potent

ginkgolide with IC<sub>50</sub> values in the high nM to the low μM range. In the FMP assay, we did not observe any selectivity for certain subtypes of the GlyR, although selectivity has recently been observed by others. This could be explained by the FMP assays being less sensitive than conventional electrophysiology and thus not allowing the detection of a weak selectivity.

A range of ginkgolide derivatives were investigated in the fluorescence-based assay, and the most potent derivatives were in the same range of activity as the native ginkgolides. These derivatives only contained modest changes, which underlines that only very minor changes of the native structures are allowed. Moreover, we confirmed the hypothesis that two lactones are essential for biological activity at GlyRs, as removal of either one of these lactones completely abolished biological activity.

A pharmacophore model was generated and a virtual screening carried out, which resulted in a number of hits. However, none of the hits tested showed activity for the GlyR at 100 μM, hence other factors not contained in the pharmacophore model must play important functions for GlyR antagonism. We propose that the structural rigidity of ginkgolides is crucial for their antagonistic properties at the GlyRs.

## Experimental Section

**Chemistry. General Procedures.** Starting materials were obtained commercially from Aldrich or Fluka, although native ginkgolides, GA–GM (1–5), were available in our laboratories from previous studies. All starting materials and solvents were used without further purification except DMF, which was stored over 3 Å molecular sieves and THF, which was distilled under N<sub>2</sub> from Na/benzophenone. <sup>1</sup>H NMR and <sup>13</sup>C NMR spectra were recorded on a Varian Mercury spectrometer at 300 MHz or on a Varian Gemini 200 BB at 300 MHz, using CDCl<sub>3</sub> or CD<sub>3</sub>OD as solvents. Accurate mass determination was performed on a JEOL JMS-HX110/100A HF mass spectrometer using a 3-nitrobenzyl alcohol (NBA) matrix and Xe ionizing gas and all are within ±5 ppm of theoretical values.

**3,14-Didehydroginkgolide A (7).** A 50 mL round-bottom flask with reflux condenser was charged with GA (1, 100 mg, 0.25 mmol) dissolved in pyridine (2 mL), and phosphorus oxychloride (41 mg, 0.27 mmol) was added to the solution at 0 °C. After 15 min the solution was heated to 50–60 °C for 2 h during which the reaction mixture darkened. After being stirred at room temperature for 14 h, the mixture was carefully poured onto ice. The precipitated product was filtered off and washed with water and dried in vacuo to give **7** (66 mg, 68%). Analytical data as previously described.<sup>28</sup>

**10-Acetoxy-ginkgolide B (10).** A 50 mL round-bottom flask with reflux condenser was charged with GB (2, 20 mg, 0.1 mmol) dissolved in acetyl anhydride (1 mL) and pyridine (1 mL). The solution was heated to 50–60 °C for 2 h. Water (1 mL) was added and the solvents were removed in vacuo. The residue was purified by flash chromatography (EtOAc/hexanes, 1:1) to give **10** (36 mg, 82%). Analytical data as previously described.<sup>29</sup>

**10-Methoxy-ginkgolide C (12).** A 50 mL round-bottom flask with reflux condenser was charged with GC (3, 40 mg, 0.09 mmol) dissolved in acetonitrile (1 mL). Potassium carbonate (14 mg, 0.1 mmol) and sodium iodide (15 mg, 0.1 mmol) were added to the solution. After 15 min, methyl iodide (28 mg, 0.2 mmol) was added and the solution was heated to 90 °C for 1 h. After the mixture was cooled to room temperature, water (5 mL) was added and the mixture was extracted with EtOAc (3 × 10 mL). The organic phase was washed with water (3 × 20 mL) and brine (3 × 20 mL) and dried over MgSO<sub>4</sub>. The organic solvents were evaporated, and the crude product was dried in vacuo. The product was purified by flash chromatography (EtOAc/hexanes 1:1) to give **12** (20 mg, 43%). Analytical data as previously described.<sup>26</sup>

**10-Methoxymethoxy-ginkgolide A (13).** A 50 mL round-bottom flask with reflux condenser was charged with GA (1, 40 mg, 0.1 mmol) dissolved in acetonitrile (1 mL). Potassium carbonate

(14 mL, 0.1 mmol) and sodium iodide (15 mg, 0.1 mmol) were added to the solution. After 15 min, methoxymethyl chloride (16 mg, 0.2 mmol) was added and the solution was heated to 90 °C for 1 h. After the mixture was cooled to room temperature, water (5 mL) was added and the mixture was extracted with EtOAc (3 × 10 mL). The organic phase was washed with water (3 × 20 mL) and brine (3 × 20 mL) and dried over MgSO<sub>4</sub>. The organic solvents were evaporated, and the crude product was dried in vacuo. The product was purified by flash chromatography (EtOAc/hexanes 1:1) to give **13** (34 mg, 71%). Analytical data as previously described.<sup>26</sup>

**1,2;3,14-Dianhydro-ginkgolide C (14).** A 50 mL round-bottom flask with reflux condenser was charged with a solution of GC (3, 50 mg, 0.1 mmol) in pyridine (1 mL). Phosphorus oxychloride (30 mg, 0.2 mmol) was added to the solution at 0 °C. After 15 min, the solution was heated to 50–60 °C for 2 h during which time the reaction mixture darkened. After being stirred at room temperature for 14 h, the mixture was carefully poured onto ice. The precipitated product was filtered, washed with water, and dried in vacuo to give **14** (27 mg, 68%). Analytical data as previously described.<sup>25</sup>

**7-Oxo-ginkgolide C (33).** A 50 mL round-bottom flask was charged with GC (3, 20 mg, 0.05 mmol) dissolved in acetone (1 mL). Chromium(VI) oxide (8 mg, 0.08 mmol) was added to the solution. After being stirred at room temperature for 2 h, the precipitate was filtered off and washed with acetone. The organic solvents were removed, and the crude product was dried in vacuo. The product was purified by flash chromatography (EtOAc/hexanes 1:1) to give **33** (15 mg, 68%). Analytical data as previously described.<sup>32</sup>

Compounds **6**, **8**, **9**, **11**, and **15–21** were from previous studies.<sup>24–27</sup>

Compounds **22–24** were those synthesized by Ishii et al.<sup>30</sup>

Compounds **25–32** and **34** were those synthesized by Vogensen et al.<sup>31</sup>

**In Vitro Pharmacology. Materials.** Culture media, serum, antibiotics, and buffers for the cell culture were obtained from Invitrogen (Paisley, UK). The cDNAs for the human α1 and β GlyR subunits were kind gifts from Professor Peter R. Schofield (Garvan Institute of Medical Research, Sydney, New South Wales, Australia), and the cDNA encoding the human α2 GlyR was a kind gift from Professor Heinrich Betz (Max-Planck-Institute for Brain Research, Frankfurt, Germany).

**Cell Culture.** The construction and pharmacological characterization of HEK293 cell lines stably expressing the GlyR subtypes α1, α1β, and α2 has been described previously.<sup>33,34</sup> Briefly, the cell lines were maintained at 37 °C in a humidified 5% CO<sub>2</sub> incubator in culture medium [Dulbecco's Modified Eagle Medium (DMEM)] supplemented with penicillin (100 U/mL), streptomycin (100 μg/mL), 10% dialyzed fetal bovine serum, 10 μM strychnine, and the appropriate antibiotics (1 mg/mL G418 for the α1 cell line, 200 μg/mL hygromycin B for the α2 cell line, and 1 mg/mL G418 and 200 μg/mL hygromycin B for the α1β cell line).<sup>33,34</sup>

**The FLIPR Membrane Potential (FMP) Assay.** The functional properties of the native ginkgolides and the derivatives were characterized at stable HEK293 cell lines expressing α1, α1β, and α2 GlyRs in the FMP assay according to the protocol of the manufacturer (Molecular Devices, Crawley, UK). The cells were split into poly-D-lysine-coated black 96-well plates (BD Biosciences, Bedford, MA) in culture medium supplemented with the appropriate antibiotics. After a 16–24 h time period, the medium was aspirated and the cells were washed with 100 μL of assay buffer [Hanks buffered saline solution supplemented with 20 mM HEPES, pH 7.4]. A 100 μL amount of assay buffer containing loading dye was added to each well (in the antagonist experiments, various concentrations of the antagonists were dissolved in the buffer), and the plate was incubated at 37 °C in a humidified 5% CO<sub>2</sub> incubator for 30 min. The plate was assayed in a NOVostar plate reader (BMG Labtechnologies, Offenburg, Germany) measuring emission [in fluorescence units (FU)] at 560 nm caused by excitation at 530 nm before and up to 1 min after addition of 25 μL of glycine solution. For the antagonist experiments, EC<sub>75</sub>–EC<sub>90</sub> concentrations

of glycine were used (200  $\mu\text{M}$  glycine for the  $\alpha 1$  and  $\alpha 1\beta$  GlyR cell lines and 500  $\mu\text{M}$  glycine for the  $\alpha 2$  GlyR cell line). The experiments were performed in duplicate at least three times for each compound. Concentration–response curves for agonists and antagonists in the FMP assay were constructed based on the maximal responses at different concentrations of the respective ligands. The curves were generated by non-weighted least-squares fits using the program KaleidaGraph 3.6 (Synergy Software).

**Electrophysiology.** The  $\alpha 1$  GlyR-HEK293 cells were split into poly-D-lysine-coated 35 mm Petri dishes containing culture medium supplemented with the appropriate antibiotics and with glass coverslips at the bottom. After a 16–24 h time period, a cover slip with cells was transferred to a recording chamber with extracellular recording solution at room temperature (20–22 °C) on the stage of Olympus BX50WI microscope (Olympus, Japan). The extracellular solution contained (in mM) the following: NaCl 140, KCl 3.5,  $\text{Na}_2\text{HPO}_4$  1.25,  $\text{MgSO}_4$  2,  $\text{CaCl}_2$  2, glucose 10, and HEPES 10; pH 7.35. Individual cells were approached with micropipettes of 2–3 M $\Omega$  resistance manufactured from 1.5 mm o.d. glass (World Precision Instruments, FA). The intrapipette solution contained (in mM) the following: KCl 140,  $\text{MgCl}_2$  1,  $\text{CaCl}_2$  1, EGTA 10, MgATP 2, and HEPES 10; pH 7.3. Standard patch-clamp techniques<sup>35</sup> in voltage clamp mode were used to record in the whole-cell configuration using an EPC-9 amplifier (HEKA, Germany). A clamping potential of –60 mV was used. Series resistance was 60–80% compensated. Whole-cell currents were recorded on computer hard disk and on a DTR-1205 DAT recorder (BioLogic, France) and analyzed subsequently using Pulse software (HEKA, Germany).

The native ginkgolides were premixed at the required concentrations in extracellular solution. When necessary, the compounds were initially dissolved in DMSO and then diluted with extracellular solution to final concentrations of DMSO of less than 0.2%. This concentration of DMSO was in itself without effect on membrane currents. An extracellular solution containing ginkgolides and/or glycine was applied using a gravity-fed seven-barrelled perfusion pipet (List, Germany) ending approximately 100  $\mu\text{m}$  from the recorded cell. By switching application from one barrel to another, the extracellular solution surrounding the cell was exchanged with a time constant of  $\sim 50$  ms. Glycine alone or premixed with ginkgolides was applied for 5 s every 1 min. Between these drug applications, ABSS (without ginkgolides or glycine) was applied from one of the barrels in order to quickly remove ginkgolides or glycine from the cell. In ginkgolide concentration–inhibition experiments, glycine at approximately  $\text{EC}_{90}$  (300  $\mu\text{M}$ ) was initially applied alone at 1 min intervals to establish a control level. Subsequently a mixture of ginkgolide and glycine was applied every 1 min until a new stable response level was reached. Then glycine was applied alone every 1 min until a stable response level was reached again, and the next ginkgolide concentration was tested. Within the 5 s of ginkgolide or glycine application, the responses always peaked or reached a stable maximum plateau. Responses were quantified by measuring the maximum currents recorded during application of ginkgolides or glycine. For the glycine concentration–response relationship the equation:

$$I = I_{\max} / (1 + \text{antilog}((\log \text{EC}_{50} - A)n_H))$$

was fitted to the experimental data, where  $I$  is the membrane current,  $A$  the logarithm of the glycine concentration,  $I_{\max}$  is the maximum current that glycine can induce,  $\text{EC}_{50}$  is the glycine concentration eliciting 50% of  $I_{\max}$ , and  $n_H$  is the Hill coefficient. For ginkgolide concentration–inhibition curves the equation

$$I = I_0 / (1 + \text{antilog}((B - \log \text{IC}_{50})n_H))$$

was fitted to the data.  $I$  is the current,  $I_0$  the current induced by 300  $\mu\text{M}$  glycine alone,  $B$  the logarithm of the ginkgolide concentration,  $\text{IC}_{50}$  the concentration of ginkgolide that reduces the current to 50% of  $I_0$ , and  $n_H$  is the Hill coefficient. Data were described using mean and 95% confidence intervals.

**Virtual Screening.** A virtual screening experiment was set up in MOE (Molecular Operating Environment, version 2004.03, Chemical Computing Group, Montreal, Quebec, Canada). Optimized geometries were calculated using the built-in mmff94x force field and the GB/SA continuum solvent model. Superimpositions of compounds were carried out using the built-in function in MOE, by fitting four donor–acceptor interactions and a single hydrophobic interaction feature. Virtual screening was conducted on a database consisting of ca. 300 000 compounds from commercial vendors, converted to 3D by the conformational import module in MOE using default settings. Thirty one hits were found, and 27 of these compounds were purchased (Supporting Information) and tested, according to the procedure described in the preceding section.

**Acknowledgment.** The authors wish to thank Drs. Schofield and Betz for their generous gifts of the GlyR cDNAs. A.A.J. was supported by the Lundbeck Foundation. K.N. would like to acknowledge NIH (GM MH068817) for financial support.

**Supporting Information Available:** Structures of the 27 compounds that were purchased and tested for activity at GlyR. This material is available free of charge via the Internet at <http://pubs.acs.org>.

## References

- DeFeudis, F. V. *Ginkgo biloba extract (EGb 761): from chemistry to clinic*; Ullstein Medical: Wiesbaden, 1998; p 401.
- DeFeudis, F. V.; Drieu, K. *Ginkgo biloba extract (EGb 761) and CNS functions: basic studies and clinical applications*. *Curr. Drug Targets* **2000**, *1*, 25–58.
- Strømgaard, K.; Vogensen, S. B.; Nakanishi, K. *Ginkgo biloba*. In *Encyclopedia of Dietary Supplements*; Coates, P., Ed.; Marcel Dekker: New York, 2005, pp 249–257.
- McKenna, D. J.; Jones, K.; Hughes, K. Efficacy, safety, and use of *Ginkgo biloba* in clinical and preclinical applications. *Altern. Ther.* **2001**, *7*, 70–90.
- Peskind, E. R. Pharmacologic approaches to cognitive deficits in Alzheimer's disease. *J. Clin. Psychiatry* **1998**, *59*, 22–27.
- Simonson, W. Promising agents for treating Alzheimer's disease. *Am. J. Health-Syst. Pharm.* **1998**, *55*, S11–S16.
- (a) Strømgaard, K.; Nakanishi, K. Chemistry and biology of terpene trilactones from *Ginkgo biloba*. *Angew. Chem., Int. Ed.* **2004**, *43*, 1640–1658; (b) Nakanishi, K. Terpene trilactones from *Ginkgo biloba*: From ancient times to the 21<sup>st</sup> century. *Bioorg. Med. Chem.* **2005**, *13*, 4987–5000.
- Strømgaard, K. Medicinal chemistry of ginkgolides from *Ginkgo biloba*. *Medicinal Chemistry of Bioactive Natural Products*; John Wiley & Sons: New York, 2006; pp 301–323.
- Strømgaard, K.; Suehiro, M.; Nakanishi, K. Preparation of a tritiated ginkgolide. *Bioorg. Med. Chem. Lett.* **2004**, *14*, 5673–5675.
- Suehiro, M.; Simpson, N. R.; van Heertum, R. L. Radiolabeling of ginkgolide B with <sup>18</sup>F. *J. Labelled Compd. Radiopharm.* **2004**, *47*, 485–491.
- Suehiro, M.; Simpson, N. R.; Underwood, M.; Castrillon, J.; Nakanishi, K.; van Heertum, R. L. In vivo biodistribution of ginkgolide B, a constituent of *Ginkgo biloba*, visualized by microPET. *Planta Med.* **2005**, *71*, 622–627.
- Kondratskaya, E. L.; Lishko, P. V.; Chatterjee, S. S.; Krishtal, O. A. BN52021, a platelet factor antagonist, is a selective blocker of glycine-gated chloride channel. *Neurochem. Int.* **2002**, *40*, 647–653.
- Kondratskaya, E. L.; Krishtal, O. A. Effects of *Ginkgo biloba* extract constituents on glycine-activated strychnine-sensitive receptors in hippocampal pyramidal neurons of the rat. *Neurophysiology* **2002**, *34*, 155–157.
- Ivic, L.; Sands, T. T. J.; Fishkin, N.; Nakanishi, K.; Kriegstein, A. R.; Strømgaard, K. Terpene trilactones from *Ginkgo biloba* are antagonists of cortical glycine and GABA<sub>A</sub> receptors. *J. Biol. Chem.* **2003**, *278*, 49279–49285.
- Betz, H.; Harvey, R. J.; Schloss, P. Structures, diversity and pharmacology of glycine receptors and transporters. *Pharmacology of GABA and glycine neurotransmission*; Springer-Verlag: Berlin, 2001.
- Lynch, J. W. Molecular structure and function of the glycine receptor chloride channel. *Physiol. Rev.* **2004**, *84*, 1051–1095.
- Chattipakorn, S. C.; McMahon, L. L. Pharmacological characterization of glycine-gated chloride currents recorded in rat hippocampal slices. *J. Neurophysiol.* **2002**, *87*, 1515–1525.
- Kondratskaya, E. L.; Betz, H.; Krishtal, O. A.; Laube, B. The  $\beta$  subunit increases the ginkgolide B sensitivity of inhibitory glycine receptors. *Neuropharmacology* **2005**, *49*, 945–951.

- (19) Kondratskaya, E. L.; Fisyunov, A. I.; Chatterjee, S. S.; Krishtal, O. A. Ginkgolide B preferentially blocks chloride channels formed by heteromeric glycine receptors in hippocampal pyramidal neurons of rat. *Brain Res. Bull.* **2004**, *63*, 309–314.
- (20) Hawthorne, R.; Cromer, B. A.; Ng, H.-L.; Parker, M. W.; Lynch, J. W. Molecular determinants of ginkgolide binding in the glycine receptor pore. *J. Neurochem.* **2006**, *98*, 395–407.
- (21) Huang, S. H.; Duke, R. K.; Chebib, M.; Sasaki, K.; Wada, K.; Johnston, G. A. R. Ginkgolides, diterpene trilactones of Ginkgo biloba, as antagonists at recombinant  $\alpha_1\beta_2\gamma_2L$  GABA<sub>A</sub> receptors. *Eur. J. Pharmacol.* **2004**, *494*, 131–138.
- (22) Chatterjee, S. S.; Kondratskaya, E. L.; Krishtal, O. A. Structure-activity studies with Ginkgo biloba extract constituents as receptor-gated chloride channel blockers and modulators. *Pharmacopsychiatry* **2003**, *36* (Suppl. 1), S68–S77.
- (23) Jaracz, S.; Nakanishi, K.; Jensen, A. A.; Strømgaard, K. Ginkgolides and glycine receptors: a structure-activity relationship study. *Chem. Eur. J.* **2004**, *10*, 1507–1518.
- (24) Weinges, K.; Schick, H.; Pritzkow, H. Chemistry of ginkgolides, VII. Preparation and crystal structure analysis of a secondary ozonide from ginkgolide A. *Liebigs Ann. Chem.* **1997**, 991–993.
- (25) Nakanishi, K. The ginkgolides. *Pure Appl. Chem.* **1967**, *14*, 89–113.
- (26) Hu, L.; Chen, Z.; Cheng, X.; Xie, Y. Chemistry of ginkgolides: structure-activity relationship as PAF antagonists. *Pure Appl. Chem.* **1999**, *71*, 1153–1156.
- (27) Hu, L.; Chen, Z.; Xie, Y.; Jiang, H.; Zhen, H. Alkyl and alkoxy-carbonyl derivatives of ginkgolide B: synthesis and biological evaluation of PAF inhibitory activity. *Bioorg. Med. Chem.* **2000**, *8*, 1515–1521.
- (28) Weinges, K.; Rümmler, M.; Schick, H.; Schilling, G. Chemistry of the ginkgolides, V. On the preparation of the ginkgolide skeleton. *Liebigs Ann. Chem.* **1993**, 287–291.
- (29) Jaracz, S.; Strømgaard, K.; Nakanishi, K. Ginkgolides: Selective acetylations, translactonization, and biological evaluation. *J. Org. Chem.* **2002**, *67*, 4623–4626.
- (30) Ishii, H.; Dzyuba, S. V.; Nakanishi, K. Lactone-free ginkgolides via regioselective DIBAL-H reduction. *Org. Biomol. Chem.* **2005**, *3*, 3471–3472.
- (31) Vogensen, S. B.; Strømgaard, K.; Shindou, H.; Jaracz, S.; Suehiro, M.; Ishii, S.; Shimizu, T.; Nakanishi, K. Preparation of 7-substituted ginkgolide derivatives: potent platelet activating factor (PAF) receptor antagonists. *J. Med. Chem.* **2003**, *46*, 601–608.
- (32) Corey, E. J.; Rao, K. S.; Ghosh, A. K. Intramolecular and intermolecular hydroxyl reactivity differences in ginkgolides A, B and C and their chemical applications. *Tetrahedron Lett.* **1992**, *33*, 6955–6958.
- (33) Jensen, A. A. Functional characterisation of human glycine receptors in a fluorescence-based high throughput screening assay. *Eur. J. Pharmacol.* **2005**, *521*, 39–42.
- (34) Jensen, A. A.; Kristiansen, U. Functional characterisation of the human  $\alpha 1$  glycine receptor in a fluorescence-based membrane potential assay. *Biochem. Pharmacol.* **2004**, *67*, 1789–1799.
- (35) Hamill, O. P.; Marty, A.; Neher, E.; Sakmann, B.; Sigworth, F. J. Improved patch-clamp techniques for high-resolution current recording from cells and cell-free membranes. *Pflügers Arch.* **1981**, *391*, 85–100.

JM070003N